HHS Public Access

Author manuscript

ACS Chem Neurosci. Author manuscript; available in PMC 2016 September 16.

Published in final edited form as:

ACS Chem Neurosci. 2015 September 16; 6(9): 1637–1648. doi:10.1021/acschemneuro.5b00165.

Modulating Molecular Chaperones Improves Mitochondrial Bioenergetics and Decreases the Inflammatory Transcriptome in Diabetic Sensory Neurons

Jiacheng Ma[†], **Pan Pan**[†], **Mercy Anyika**[‡], **Brian S. J. Blagg**[‡], and **Rick T. Dobrowsky**[†,*]

[†]Department of Pharmacology and Toxicology, The University of Kansas, Lawrence, Kansas 66045, United States

[‡]Department of Medicinal Chemistry, The University of Kansas, Lawrence, Kansas 66045, United States

Abstract

We have previously demonstrated that modulating molecular chaperones with KU-32, a novobiocin derivative, ameliorates physiologic and bioenergetic deficits of diabetic peripheral neuropathy (DPN). Replacing the coumarin core of KU-32 with a meta-fluorinated biphenyl ring system created KU-596, a novobiocin analogue (novologue) that showed neuroprotective activity in a cell-based assay. The current study sought to determine whether KU-596 offers similar therapeutic potential for treating DPN. Administration of 2–20 mg/kg of KU-596 improved diabetes induced hypoalgesia and sensory neuron bioenergetic deficits in a dose-dependent manner. However, the drug could not improve these neuropathic deficits in diabetic heat shock protein 70 knockout (Hsp70 KO) mice. To gain further insight into the mechanisms by which KU-596 improved DPN, we performed transcriptomic analysis of sensory neuron RNA obtained from diabetic wild-type and Hsp70 KO mice using RNA sequencing. Bioinformatic analysis of the differentially expressed genes indicated that diabetes strongly increased inflammatory pathways and that KU-596 therapy effectively reversed these increases independent of Hsp70. In contrast, the effects of KU-596 on decreasing the expression of genes regulating the production of reactive

[*]**Corresponding Author** Rick T. Dobrowsky. Mailing address: Department of Pharmacology and Toxicology, University of Kansas, 5064 Malott Hall, 1251 Wescoe Hall Dr., Lawrence, KS 66045. Phone: (785) 864-3531. Fax: (785) 864-5219. dobrowsky@ku.edu.

ASSOCIATED CONTENT

Supporting Information

Representative results from the FastQC check of the FASTQ files from one replicate in each of the four treatment groups from WT (A–D) and Hsp70 KO (E–H) mice, total CuffDiff output of all genes in each treatment group from WT mice, total CuffDiff output of all genes in each treatment group from Hsp70 KO mice, significantly activated or inhibited upstream regulator genes identified by pathway analysis for diabetic WT and Hsp70 KO mice in the absence and presence of drug treatment, mitochondrial genes that were differentially expressed in diabetic Hsp70 KO mice treated with KU-596, and PCR primer sequences. The Supporting Information is available free of charge on the ACS Publications website at DOI: 10.1021/acschemneuro.5b00165.

Accession Codes

All raw FASTQ files have been deposited to the NCBI Sequence Read Archive and should be accessible via accession number SRX1085145.

Author Contributions

J.M. and R.T.D. participated in research design; J.M. and P.P. conducted experiments; M.A. and B.S.J.B. contributed reagents; J.M., P.P., and R.T.D. performed data analysis; J.M. and R.T.D. contributed to the writing of the manuscript.

The authors declare the following competing financial interest(s): R.T.D. and B.S.J.B. declare a financial interest through a licensing agreement of KU-596 with Reata Pharmaceuticals.

oxygen species were more Hsp70-dependent. These data indicate that modulation of molecular chaperones by novologue therapy offers an effective approach toward correcting nerve dysfunction in DPN but that normalization of inflammatory pathways alone by novologue therapy seems to be insufficient to reverse sensory deficits associated with insensate DPN.

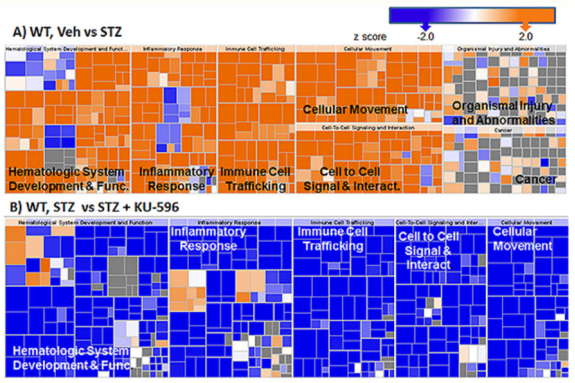

Keywords

Bioenergetics; diabetic neuropathy; inflammation; molecular chaperones; oxidative stress; RNA Seq

---

Diabetes is a major public health concern in the United States and worldwide. The number of diabetic patients is estimated to exceed 500 million by 2030,[1] and greater than half of these individuals are likely to develop diabetic peripheral neuropathy (DPN), the most common diabetic complication. Patients with both type 1 and type 2 diabetes can develop either a painful or an insensate peripheral neuropathy that greatly reduces quality of life. Unfortunately, despite our increased understanding of the etiology of DPN, few FDA-approved treatments exist for managing painful DPN, and no approved treatments are available to ameliorate insensate DPN. Currently, the most effective approach for decreasing the risk of developing or ameliorating DPN is tight glycemic control. However, prolonged tight glycemic control is difficult to obtain for the average patient and is more effective in type 1 versus type 2 diabetics.[2,3]

The onset of insensate DPN is associated with numerous pathophysiological changes that involve increased flux of glucose through the polyol pathway, enhanced protein modification by *N*-acetylglucosamine, production of advanced glycation end products (AGEs), increased oxidative and nitrosative stress, protein kinase C activation, altered growth factor signaling, and changes in mitochondrial bioenergetics (mtBE). Many excellent reviews have characterized the progress in elucidating mechanisms that contribute to the development of DPN and the outcomes of pharmacologic efforts to improve disease management.[4–9] Though targeting many of these pathways has effectively reversed insensate DPN in animal models, translational success in humans has not materialized at this point. Given the complex natural history of the disease, which can develop over decades, and the uncertainty of the necessity of any one pathogenic component to disease progression at a given stage, a polypharmacy approach may prove useful. On the other hand, it is

increasingly appreciated that effective management of complex, chronic neurodegenerative diseases such as Alzheimer's disease and DPN may not necessarily require targeting a pathway or protein considered to contribute to disease progression. Alternatively, it may prove sufficiently beneficial to pharmacologically enhance the activity of endogenous neuroprotective pathways to aid neuronal recovery and to tolerate diabetic stress.[10]

Molecular chaperones such as heat shock protein 90 (Hsp90) and Hsp70 are essential for the folding or refolding of newly translated or denatured proteins. Though distinct genes, Hsp90 and Hsp70 are intimately related via the heat shock response. Hsp90 binds the transcription factor heat shock factor 1 and inhibits its transactivating capacity. Upon exposure to stress or classic N-terminal Hsp90 inhibitors, heat shock factor 1 dissociates, translocates to the nucleus, and upregulates antioxidant genes and a variety of chaperones, including Hsp70.[11] Stimulating this aspect of Hsp90 biology can have potential utility for treating neurodegenerative diseases associated with protein misfolding since an increase in Hsp70 can decrease protein aggregation in Alzheimer's[12,13] and other neurodegenerative diseases.[14–16] Hsp90 inhibitors have also been developed that bind within the ATP-binding domain in the protein's C-terminus, and we have focused on developing this class of inhibitors in treating DPN. Pharmacological modulation of Hsp90 with KU-32 (Figure 1A), a first-generation novobiocin-based, C-terminal binding drug, decreased glucose-induced death of primary sensory neurons and improved electrophysiologic, psychosensory, bioenergetic, and morphologic deficits of DPN in a Hsp70-dependent manner.[17–19]

Though KU-32 is quite efficacious in treating DPN, molecular modeling of the drug docked to the Hsp90 C-terminal binding pocket indicated that the coumarin lactone appeared too distant from Lys539 to provide complementary interactions with this residue. Additionally, the 3-amido side chain of KU-32 projected into a large hydrophobic pocket that could accommodate more flexible linkers.[20] Consequently, novologues (novobiocin analogues) were designed to contain a biphenyl scaffold that replaced the coumarin lactone of KU-32. It was hypothesized that the B-ring of the biphenyl would project into the Hsp90 C-terminal binding pocket and serve as a lead compound for further diversification. Subsequent modifications supported that substitution of electronegative atoms in the meta-position of the benzene ring had improved neuroprotective activity, potentially due to an enhanced interaction with Lys539 in the Hsp90 C-terminal binding pocket.[20] KU-596 (Figure 1B) was identified as a *meta*-3-fluorophenyl substituted novologue that exhibited an improved ED_{50} for protecting primary sensory neurons against glucotoxicity compared with KU-32.

Since KU-32 therapy was associated with a Hsp70-dependent restoration of mitochondrial respiratory capacity and reduced oxidative stress in sensory neurons,[19,21] we sought to determine whether KU-596 displays similar Hsp70-dependent efficacy in animal models of DPN. Further, since Hsp70 has numerous cytoprotective properties,[22] we hypothesized that multiple genes or gene networks within sensory neurons may contribute to the reversal of insensate DPN by KU-596 in an Hsp70-dependent manner.

The application of system biology approaches has yielded novel insight into metabolomic and genetic networks that contribute to the development of DPN in animal models of type 2 diabetes[23,24] and that distinguish humans with progressive versus nonprogressive DPN.[25]

Though the use of microarrays has successfully defined diabetes-induced changes in the peripheral nerve transcriptome, DNA microarrays have a small dynamic range and lack sensitivity for quantifying genes expressed either at low or very high levels due to background array signals or signal saturation.[26] In contrast, high throughput transcript sequencing (RNA-Seq) has a dynamic range spanning 5 orders of magnitude and permits detection of abundant and even very rare transcripts, with sufficient sequencing depth.[27] Following sequencing, the resulting reads are aligned to a reference genome and qualitative or quantitative results are obtained through bioinformatic analysis of the sequencing data.[26] Therefore, we examined transcriptomic changes within sensory neurons that contribute to the reversal of insensate DPN using the RNA-Seq approach. Collectively, these data provide novel insight into the role of mitochondrial dysfunction, oxidative stress, and inflammation in the onset and attenuation of insensate DPN and further corroborate the therapeutic potential of modulating molecular chaperones as a treatment for DPN.

RESULTS AND DISCUSSION

KU-596 Dose-Dependently Improves Sensory Function and Mitochondrial Bioenergetics in Diabetic Mice

After 14 weeks of diabetes, Swiss Webster mice displayed significantly elevated fasting blood glucose (FBG) and glycated hemoglobin (HbA1c) levels, a measure of blood glucose control over a 2–3 month period (Table 1). Diabetes also promoted a significant decrease in body weight. KU-596 treatment did not improve FBG, HbA1c, or body weight in the diabetic mice, as reported previously with KU-32. By 8 weeks of diabetes, the mice developed significant mechanical (Figure 2A) and thermal (Figure 2B) hypoalgesia. After 8 weeks of diabetes, KU-596 was administered for 6 weeks via a once per week intraperitoneal dosing at 2, 10, or 20 mg/kg. These treatments dose-dependently reversed the pre-existing psychosensory deficits. KU-596 also dose-dependently prevented the diabetes-induced deficits in motor (MNCV) and sensory (SNCV) nerve conduction velocities (Figure 2C). Since these electrophysiologic measures were not assessed prior to drug treatment, we cannot necessarily conclude that the novologue reversed any pre-existing electrophysiologic deficits, as reported with KU-32.[28]

To determine whether the changes in psychosensory function and NCV were accompanied by improvements in mtBE, sensory neurons were isolated from the L_4–L_6 lumbar ganglia after 14 weeks of diabetes; these neurons provide the axons that are affected in DPN and were improved by novologue treatment. The diabetic sensory neurons showed a significant decline in maximal respiratory capacity (MRC) in response to the protonophore FCCP. This response indicates an impaired rate of maximal respiration in the absence of the constraints imposed by the proton gradient across the inner mitochondrial membrane (Figure 3A).

Similarly, diabetes decreased spare respiratory capacity (SRC) (Figure 3B), which is an assessment of the bioenergetic reserve that is available to respond to cellular energy demands. Both of these bioenergetic parameters were dose-dependently improved by 6 weeks of KU-596 treatment. The ability of KU-596 to increase MRC and SRC in the diabetic mice suggests that modulating molecular chaperones is improving the efficiency of electron transport. A few possibilities underlying this effect may be due to drug treatment

rectifying some damaging effects of prolonged hyperglycemia on proteins involved in electron transport or via improving the generation of reducing equivalents or substrate availability to the diabetic mitochondria. Thus, similar to KU-32,[21] the improvement in sensory function correlates with an increase in the bioenergetic capacity of the sensory neurons by KU-596. Of interest, the novologue also increased mitochondrial function in nondiabetic mice but had no effect on the sensory measures. Thus, this increase in mitochondrial function is not sufficient to alter nerve sensory physiology in nondiabetic mice.

KU-596 Improves Sensory Parameters in a Hsp70-Dependent Manner

In our previous studies, the neuro-protective efficacy of KU-32 in reversing the sensory and respiratory deficits required the presence of Hsp70 since neuropathic Hsp70 KO mice were insensitive to drug treatment.[21] To determine whether the efficacy of KU-596 also required stress-inducible Hsp70, C57Bl/6 and Hsp70 KO mice were rendered diabetic and after 12 weeks of diabetes, the mice were administered 20 mg/kg KU-596 weekly via oral gavage for 4 weeks. Both genotypes developed extensive diabetes as shown by a loss of body weight and increase in FBG and HbA1c levels (Table 2). Similar to the Swiss Webster mice, none of these parameters were affected by novologue therapy. By 12 weeks of diabetes, wild-type (WT) and Hsp70 KO diabetic mice showed significant decreases in their response to mechanical (Figure 4A,B) or thermal (Figure 4C,D) stimuli indicating that Hsp70 is not necessary to develop insensate DPN. Four weeks of KU-596 treatment significantly reversed the sensory hypoalgesia in WT mice (Figure 4A,C) but not the Hsp70 KO mice (Figure 4B,D). Thus, the above results suggest that the novologue also reverses sensory deficits of DPN in a Hsp70-dependent manner.

RNA-Seq Analysis of Sensory Neurons

To determine the transcriptome changes within sensory neurons that may contribute to the more complete recovery of function that occurs with 6–8 weeks of treatment with KU-596, the mice were only treated for 4 weeks. To this end, NCV or sensory neuron bioenergetics were not assessed in these animals to avoid any potential changes in transcript expression for subsequent RNA-Seq analysis. RNA was isolated from the L_4–L_6 lumbar DRG of two mice per treatment with three to five biologic replicates per group for RNA-Seq analysis. In the WT mice, 23 112 genes were detected by RNA-Seq and 39.6% were expressed too low or were not detected in all the treatments, yielding 13 959 genes that were statistically analyzed. Of these genes, 343 were significantly modified in diabetic WT compared with control neurons, with the majority showing an increase in expression. KU-596 treatment significantly altered the expression of 174 genes in diabetic sensory neurons and 42 genes in control sensory neurons. Among the subset of transcripts that were significantly altered by diabetes in the absence or presence of KU-596, 67/70 had their expression decreased by the drug in the diabetic neurons. Impressively, KU-596 consistently decreased transcript expression in an almost quantitatively opposite direction (Figure 5A). Surprisingly, only 101 were genes were significantly modified in sensory neurons from the diabetic Hsp70 KO mice. Moreover, KU-596 treatment significantly altered 242 genes in these mice despite having no effect on improving the sensory measures; the drug altered 37 genes in control sensory neurons from the Hsp70 KO mice. Among the shared genes, 31 were increased in

diabetic Hsp70 KO neurons and decreased by KU-596 treatment (Figure 5B). Interestingly, the magnitude of the normalization in gene expression was similar to the efficacy of KU-596 in diabetic WT mice. Thus, the drug does not require Hsp70 to correct the expression of all genes, and only 8 genes were similarly affected by KU-596 in both WT and Hsp70 KO mice (red in Figure 5). Supporting Tables 1 and 2, Supporting Information, provide the CuffDiff output (see Methods) for all treatments in WT and Hsp70 KO mice, respectively. The tables can be filtered to readily indicate the genes that showed a significant differential expression ($q \leq 0.05$).

To validate the RNA-Seq analysis, several genes that were altered in both the untreated diabetic and STZ + KU-596 treated WT mice were chosen for qRT-PCR analysis in independent samples. Due to limits in the amounts of RNA obtained from each DRG sample, seven genes with an FPKM ≥ 5 (see Methods) were selected for qRT-PCR analysis (*arhgdib, fabp4, fkbp5, lcn2, ltf, s100a8, txnip*). Though only *txnip* and *fkbp5* showed statistical significance due to the variability in the small sample size ($n = 3$ in each group), the other selected genes followed similar trends in the qRT-PCR analysis compared with the RNA-Seq data (Figure 6). Collectively, these data suggest that KU-596 can reverse transcriptome alterations in the sensory neurons of type 1 diabetic mice.

Novologue Therapy Improves Markers of Inflammation

To gain insight into biological processes that were altered by diabetes and normalized by novologue therapy, pathway analysis of the differentially expressed transcripts revealed that inflammation was a top biologic process induced by diabetes (Figure 7A). The change in gene expression in the untreated diabetic group relative to nondiabetic mice was predicted to upregulate inflammatory responses, which supports the involvement of inflammation in the pathogenesis of DPN. Other enriched canonical pathways involved chemotaxis, immune cell trafficking, and production of nitric oxide and reactive oxygen species (ROS), which are also indicative of altered inflammatory responses.[29]

KU-596 broadly reversed the diabetes-induced activation of inflammatory pathways (Figure 7B). Numerous cytokines and transcriptional regulators that were predicted to be activated by diabetes showed an almost quantitative reversal by novologue therapy in WT mice (Supporting Table 3, Supporting Information). These data provide the first evidence that modulation of inflammatory pathways might contribute to the neuroprotective effects of KU-596.

Despite the difference between the gene sets affected in the Hsp70 KO and WT mice, inflammation was still among the top canonical pathways significantly enriched and increased in activity in the diabetic Hsp70 KO mice (Figure 7C). However, the increase in inflammatory pathways was not as robust in the diabetic Hsp70 KO mice. This may be related to a role of Hsp70 in the stimulation of pro-inflammatory cytokine production and recruitment of macrophages and monocytes.[30,31] Unexpectedly, inflammatory pathways were also broadly downregulated in diabetic Hsp70 KO mice treated with KU-596 (Figure 7D and Supporting Table 3, Supporting Information). Thus, KU-596 decreased the inflammatory response in diabetic sensory neurons through one or more Hsp70-independent pathways, but this was not sufficient to improve the sensory deficits (Figures 4B,D).

Recent studies suggest that Hsp70 is actively released into the extracellular milieu to promote innate and adaptive immune responses under stress conditions[32] and that the physiological function of Hsp70 largely depends on the location of the protein.[33] Consistent with this premise, Hsp70.1-deficent mice were more resistant to developing autoimmune encephalomyelitis, suggesting the involvement of Hsp70.1 in promoting an effective myelin oligodendrocyte glycoprotein T cell response.[34] Increased extracellular Hsp70 has been associated with inflammatory and oxidative stress conditions,[35] whereas increased intracellular Hsp70 confers cellular protection through anti-inflammatory effects.[36] In this regard, increased concentrations of extracellular Hsp70 and decreased concentrations of intracellular Hsp70 have been reported in type 2 diabetic patients.[37] Conceivably, extracellular Hsp70 may mediate the activation of inflammatory pathways in WT diabetic sensory neurons, which may contribute to the weaker transcriptomic changes of these pathways in the diabetic Hsp70 KO mice.

Among the inflammation genes, CD163 is a macrophage and monocyte scavenger receptor that mediates endocytosis of haptoglobin-hemoglobin complexes. CD163 is a macrophage-derived low-grade inflammation marker that indicates a level of macrophage activation.[38] Though macrophages have been detected in nerve after 8 weeks of diabetes,[39] whether they are a cause or consequence of the developing DPN is unclear. However, a recent case-control study involving a small number of type 2 diabetic patients indicated that an increase in soluble CD163 levels in cerebrospinal fluid and serum was associated with impaired large fiber function and incidence of DPN.[40] In the current study, CD163 was increased ~3-fold in WT diabetic sensory neurons and decreased ~2-fold by KU-596 treatment (Supporting Table 1, Supporting Information). CD163 was also upregulated 1.4-fold in diabetic Hsp70 KO neurons, but this did not quite reach statistical significance ($q < 0.06$). However, qPCR showed a significant increase in CD163 expression ((3.6 ± 1.6)-fold, Veh vs STZ; $p < 0.05$) in the diabetic Hsp70 KO mice, and this increase was unaffected by KU-596 when assessed by qPCR ((4.3 ± 0.7)-fold, Veh vs STZ + KU-596) or RNA Seq (1.7-fold, Veh vs STZ + KU-596). Therefore, Hsp70 does not necessarily have a role in increasing the expression of CD163 in diabetic macrophages, but the novologue may decrease this inflammatory marker in a Hsp70-dependent manner. Given the putative link that type 2 diabetic patients with neuropathy show a greater increase in serum CD163 levels than diabetic individuals without neuropathy, the ability of KU-596 therapy to decrease its expression may provide a biomarker for drug efficacy.[40] However, since the mean duration of diabetes in this pool of type 2 diabetics was 13 years, it is not possible to determine whether CD163 may be a marker for diabetic damage or if early activation of macrophages may contribute to the large fiber impairment. Moreover, whether the relationship between serum CD163 levels and markers of neuropathy may extend to type 1 diabetic patients with DPN remains to be clarified.

Although inflammation is strongly associated with the development of DPN in mouse models of type 2 diabetes,[24,41] an increase in inflammatory markers such as TNFα and IL-1β in DRG of type 1 diabetic rats has also been noted. Induction of Hsp70 following weekly exercise correlated with a decrease in these inflammatory mediators and an improvement in measures of painful neuropathy.[42,43] Interestingly, inflammatory markers

such as neuropeptide Y (NPY) and NOX2 (NADPH oxidase 2 or Cybb, cytochrome *b*(245) subunit *β*) were increased at the protein or gene expression level in bone marrow of type 1 diabetic rats. These inflammatory markers were decreased by treatment with an aldose reductase inhibitor plus lipoic acid, which correlated with an improvement in measures of a sensory neuropathy.[44] These genes were similarly increased by diabetes in our study and decreased by KU-596. Thus, inflammation may be a contributing feature to both painful and insensate diabetic neuropathy that is amenable to chaperone modulation. However, a role of inflammation in contributing to DPN in murine models of type 1 diabetes needs to be cautiously assessed as it may be affected by genotypic variations in the C57Bl/6 strains that are used. For example, the primary genotypic variant between C57Bl/6J and C57Bl/6N strains is deletion of exons 7–12 for the gene encoding the mitochondrial enzyme nicotinamide nucleotide transhydrogenase (*nnt* gene) in C57Bl/6J mice. The absence of this gene differentially affects glucose homeostasis in response to a high fat diet compared with C57Bl/6N mice.[45] Additionally, the loss of *nnt* promotes a redox imbalance in mitochondria that can increase susceptibility to oxidative stress and apoptosis.[46] Thus, *nnt* deletion may impact the gene expression profile with this strain in diabetic and prediabetic peripheral neuropathies. Our current and past studies have used the C57Bl/6N as our wild-type line, which expresses a functional *nnt* gene. Examination of the RNA Seq alignments between the WT and Hsp70 KO mouse showed no differences in the detection of *nnt* exons and the FPKM values were essentially identical between the strains. Thus, it is unlikely that that activation of inflammatory or oxidative stress responses in our diabetic mice is confounded by this gene deletion.

Hsp70 Is Associated with a Decrease in Genes Linked to the Production of Oxidative Stress

Not unexpectedly, another over-represented biologic process in the diabetic WT (Figure 8A) and Hsp70 KO (Figure 8C) sensory neurons comprised genes involved in the production of ROS. However, KU-596 treatment was predicted to significantly normalize the expression of these genes only in the diabetic WT mice (Figure 8B), suggesting that the drug may reduce oxidative stress in a Hsp70-dependent manner. Oxidative stress is considered to be an essential pathogenic mechanism for DPN.[47–49] Hyperglycemia changes multiple biochemical and metabolic pathways that can converge at the level of ROS production to contribute to the development and progression of DPN.[50] For example, Cybb (NOX2), a superoxide generating enzyme that forms ROS,[51] increased ~2-fold in diabetic WT sensory neurons and was reduced ~2-fold by KU-596 treatment. Thioredoxin interacting/inhibiting protein (Txnip) is induced by diabetes,[52] and it promotes oxidative stress through interacting with thioredoxin and blocking its ROS scavenging activity.[53] Txnip was upregulated ~2-fold in diabetic neurons and down-regulated about 1.4-fold by KU-596. Though diabetes significantly increased the expression of Txnip in the Hsp70 KO DRG by about 1.4-fold, this was unaffected by KU-596 treatment, which was validated by qPCR as well (data not shown). Therefore, limiting ROS production and reducing oxidative stress in the sensory neurons might represent an important Hsp70-dependent pathway through which KU-596 exhibits efficacy on reversing sensory deficits of DPN. Though the exact mechanism through which Hsp70 modulates ROS production remains to be determined, its overexpression has been associated with protection against age-related oxidative stress.[54]

Mechanistically, this may be a rather direct effect on the neurons rather than by indirectly decreasing inflammation since we have shown that KU-32 increased the translation of MnSOD and decreased oxidative stress using *in vitro* cultures of hyperglycemically stressed rat embryonic sensory neurons.[19]

KU-596 and the Mitochondrial Transcriptome

KU-596 (Figure 3) and KU-32[21] both reversed mtBE deficits in diabetic sensory neurons. Thus, one expectation was that transcriptome analysis would reveal gene clusters connecting to aspects of mitochondrial function. However, none of the genes involved in cellular bioenergetic activities were significantly altered in the STZ + Veh or STZ + KU-596 groups of WT mice. This observation suggests that the alterations in mtBE in the diabetic sensory neurons may not be due to transcriptome changes in genes involved in mitochondrial function. Because our prior proteomic study reported that diabetes decreased the expression of mitochondrial proteins,[55] diabetes and KU-596 may exert their effects on mtBE at the protein level. Modulation of molecular chaperones may exert effects on mitochondrial function post-translationally through refolding of damaged proteins, by facilitating protein import into mitochondria, or by decreasing oxidative stress. In addition, it has been suggested that inflammatory signaling leads to changes in the phosphorylation state of mitochondrial proteins, which results in an inhibition of respiratory chain activity, a reduction of the mitochondrial membrane potential, and consequently a lack of energy production.[56] In this regard, the effect of KU-596 to improve mtBE might be partially attributed to its effects in ameliorating inflammatory signaling in the sensory neurons.

Curiously, KU-596 decreased the transcription of several mitochondrial genes in diabetic Hsp70 KO sensory neurons even though only one these genes (*ndufb2*) was significantly increased in diabetic mice that did not receive the drug (Supporting Table 4, Supporting Information). This effect was not observed in diabetic WT mice or nondiabetic Hsp70 KO treated with the drug. Though mtBE was not measured in the diabetic Hsp70 KO mice treated with KU-596, the decrease in mRNA levels of these mitochondrial proteins was unlikely to result in changes in mitochondrial respiration since KU-32 did not decrease mtBE in sensory neurons isolated from diabetic Hsp70 KO mice.[21] Although the underlying reason is unknown, this effect of KU-596 on mitochondrial transcripts might be associated with a role of Hsp90 in mitochondrial protein turnover. In the absence of Hsp70, the effects of KU-596 on transcriptome changes may be exerted through inhibiting Hsp90 activity. A previous *in vitro* study showed that Hsp90 inhibition led to post-translational accumulation of several mitochondrial oxidative phosphorylation complex subunits without corresponding changes in mRNA abundance.[57] Thus, the decrease in transcription observed in our study might be an innate response to the accumulation of these mitochondrial proteins due to inhibition of Hsp90 over the 4 weeks of drug treatment. As an essential molecular chaperone that assures the correct folding and maturation of a number of cellular proteins, Hsp90 inhibition leads to a global repression of protein synthesis and an increase in the degradation of its client proteins.[58] This finding is consistent with our observation that KU-596 also decreased a subset of 25 ribosomal proteins only in diabetic Hsp70 KO sensory neurons. A recent proteomics study using human T cells revealed that Hsp90 inhibition resulted in the depletion of proteins involved in transcription and DNA damage response as well as a mild

but general decrease of ribosomal proteins and other components of the protein synthesis machinery.[59] Considering these data, the differences in the gene sets affected by KU-596 in WT versus Hsp70 KO mice might be related to the distinct downstream pathways induced by drug treatment in the genotypes: whereas KU-596 exerts cytoprotective effects through Hsp70 in WT cells, the effects of KU-596 may be largely exerted through inhibiting the activity of Hsp90 in Hsp70 KO cells.

SUMMARY AND CONCLUSIONS

The current work extends our prior observations that modulating Hsp90 activity with small molecules that target the protein's C-terminal domain may provide a novel translational approach toward treating insensate DPN. KU-596 represents the next generation of novobiocin-based molecules whose efficacy in reversing symptoms of DPN requires Hsp70 and is linked to improving sensory neuron mtBE and decreasing inflammatory pathways. Though KU-596 decreased the activation of inflammatory pathways in diabetic Hsp70 KO mice, this was not sufficient to rescue the sensory deficits. Thus, the decrease in inflammatory markers in diabetic WT mice treated with KU-596 is likely parallel to the main mechanism for improving DPN, at least in the type 1 diabetes that is modeled in the current work. On the other hand, the decrease in genes linked to the production of ROS was more Hsp70-dependent, suggesting that this may underlie the improvement in mtBE and sensory function. Nonetheless, the decrease in inflammatory pathways may be a critical contributing feature that aids neuronal tolerance to diabetic stress in response to novologue therapy.

METHODS

Materials

Streptozotocin (STZ), carbonylcyanide-4-(trifluoromethoxy)-phenylhydrazone (FCCP), oligomycin, rotenone, antimycin A, Percoll, and poly(DL)ornithine were obtained from Sigma-Aldrich (St. Louis, MO). KU-596, *N*-(2-(5-(((3*R*,4*S*,5*R*)-3,4-dihydroxy-5-methoxy-6,6-dimethyltetrahydro-2*H*–pyran-2-yl)oxy)-3′-fluoro-[1,1′-biphenyl]-2-yl)ethyl)-acetamide, was synthesized, and structural purity (>95%) was verified as described previously.[20]

Animals

Male Swiss Webster mice were purchased from Harlan Laboratories (Indianapolis, IN). Male and female wild-type (WT) C57Bl/6 and Hsp70.1/70.3 double knockout (KO) mice on a C57Bl/ 6 background (Hsp70 KO) were obtained from in-house breeding colonies. The WT mice (C57Bl/6NHsd) were originally obtained from Harlan Laboratories, and the Hsp70 KO mice were initially obtained from the Mutant Mouse Resource and Research Center. All animals were maintained on a 12-h light/dark cycle with ad libitum access to water and 7022 NIH-07 rodent chow (5.2% fat). All animal procedures were performed in accordance with protocols approved by the Institutional Animal Care and Use Committee and in compliance with standards and regulations for the care and use of laboratory rodents set by the National Institutes of Health.

Diabetes was induced in male Swiss Webster mice by an intraperitoneal injection of 100 mg/kg STZ given on two consecutive days after 6 h of fasting. Fasting blood glucose (FBG, One Touch Ultra glucometer) was determined 1 week after the second injection following 6 h of food withdrawal. Mice with FBG ≥ 290 mg/dL (16 mM) were deemed diabetic. FBG and glycated hemoglobin (HbA1c, A1c Now^{+}) were also measured at study termination. KU-596 was administered after 8 weeks of diabetes via once per week intra-peritoneal injections of 2, 10, or 20 mg/kg in 0.1 M Captisol (β-cyclodextrin sulfobutylethers; CyDex Pharmaceuticals, Lenexa, KS). Of note, the vehicle–vehicle and diabetes–vehicle mice were part of a larger dose–response comparison study between KU-32 and KU-596. However, only the dose–response profile of KU-32 has been previously published.[21]

In the RNA Seq study, diabetes was induced in 8-week-old male and female WT or Hsp70 KO mice as described above. After 12 weeks of diabetes, 20 mg/kg KU-596 in 0.1 M Captisol was given to the mice vial oral gavage (~0.2 mL) once per week for 4 weeks. Mice were randomly assigned to each of the treatments in both studies.

Psychosensory and Electrophysiologic Analyses

Mechanical sensitivity was assessed using a dynamic plantar aesthesiometer (Stoelting Inc.) fitted with a stiff monofilament that was applied to the plantar surface at an upward force of 10 g for Swiss Webster mice or 8 g for C57Bl/6 and Hsp70 KO mice. Thermal sensitivity was assessed by paw withdrawal latency to a ramping, focal heat using a Hargreaves analgesiometer (Stoelting Inc.).[21] Responses from each animal were measured four times on alternate feet and averaged. At the end point of a study, animals were anesthetized prior to measuring motor and sensory nerve conduction velocities (MNCV and SNCV) as previously described.[60] Animals were then euthanized prior to tissue collection.

Mitochondrial Bioenergetics Assessment

Oxygen consumption rate (OCR) was assessed in intact lumbar DRG sensory neurons using the XF96 extracellular flux analyzer (Seahorse Biosciences, North Billerica, MA). Lumbar sensory neurons were dissected from two to three mice and pooled together, and the neurons were isolated as previously described.[21] The cells were maintained overnight in Ham's F10 medium (6.1 mM glucose) containing 50 ng/mL nerve growth factor, 1 ng/mL neurotrophin 3 and N2 supplement without insulin (Invitrogen, Carlsbad, CA). The following day, the medium was changed to unbuffered DMEM supplemented with 1 mM sodium pyruvate and 5.5 mM D-glucose, and the cells were incubated at 37 °C for 1 h before being introduced to the XF96 analyzer. The initial readings provide a measure of the basal OCR before the addition of respiratory chain poisons.[61] The addition of oligomycin (1 μg/mL), an ATP synthase inhibitor, leads to a decrease in OCR which represents the portion of basal OCR that is coupled to ATP synthesis. The residual OCR that persists after addition of oligomycin is from uncoupled respiration (proton leak). Next, maximal respiratory capacity (MRC) was assessed by adding 1 μM FCCP, a protonophore that dissipates the proton gradient across the inner mitochondrial membrane. Nonmitochondrial respiration was then assessed by co-injection of 1 μM rotenone + 1 μM antimycin A. After the respiratory measures, the cells were harvested, and OCR values were normalized to the total protein content of each well.

Maximal respiratory capacity (MRC) and spare respiratory capacity (SRC) were quantified as described previously.[61,62]

Isolation of RNA

L_4– L_6 lumbar DRG from two animals were pooled together for the isolation of one total RNA sample. Each treatment group contained three to five biological replicates. Tissues were harvested, rapidly frozen in liquid nitrogen and stored at −80 °C. The tissue was ground in liquid nitrogen, and 900 μL of Trizol was added to each sample. RNA was isolated following the standard protocol of the Qiagen RNeasy Plus Universal Mini Kit (Qiagen, Venlo, CA). RNA quality and concentration was checked with the Agilent 2200 Tape Station (Agilent Technologies, Santa Clara, CA) and Qubit fluorometric quantitation (Life Technologies, Carlsbad, CA), respectively. RNA with an integrity number (RIN) ≥ 7 was used for RNA-Seq analysis or qRT-PCR analysis.

Illumina RNA-Seq

Total RNA (100 ng) was used to prepare cDNA libraries with the TruSeq stranded total RNA library prep kit (Illumina Inc., San Diego, CA). In general, poly(A)$^+$ containing mRNA was purified with oligo-dT attached magnetic beads. Purified mRNA was then fragmented and primed with random hexamers, which were subsequently reverse transcribed into first strand cDNA using reverse transcriptase. The RNA templates were then removed from the single-strand cDNA and a replacement strand was synthesized to generate double-strand cDNA. The double-strand cDNA was end-repaired and adenylated at the 3′ ends. For each sample, Illumina-specific adaptors that contain a unique 6 bp index sequence that identifies each sample were ligated to the 3′ adenine-tail of the fragments to permit the single read, multiplex sequencing of transcripts within each lane of the flow cell. cDNA products (~260 bp) were amplified and submitted to quality control with the Agilent 2200 Tape Station. cDNA libraries prepared from the three to five biological replicates from each treatment group were then randomly assigned to two lanes of the flow cell for subsequent single-end sequencing with a read length of 100 bases using the Illumina HiSeq 2500 System (Illumina Inc., San Diego, CA).

Bioinformatics Analysis of RNA-Seq Data

After the initial processing and demultiplexing steps with the Illumina Analysis Visual Controller software, the resulting FASTQ files were analyzed via the Galaxy Project web-based portal[63] (http://usegalaxy.org/) linked to the freely available Tuxedo Suite.[64,65] FASTQ files were quality checked using FASTQC and used ungroomed (Supporting Figure 1, Supporting Information). The files were submitted to the Tophat module to align the short read sequences to the mouse genome (mm9). The reads for each biological replicate were mapped independently and submitted to Cufflinks, which assembled and annotated the transcripts of each sample. The resulting files for all treatments were merged with the reference genome using CuffMerge. The CuffMerge output and Tophat files were loaded into the CuffDiff module to quantify significant changes in transcript expression between groups.[64,65] Gene level expression data were normalized to obtain fragments per kb per million aligned reads (FPKM), and the log 2-fold change between groups was calculated

based on the FPKM data. A *t* test was used to calculate the *p*-value for differential gene expression in the Cuffdiff module and the resulting *p*-values were adjusted by the Benjamini–Hochberg method to compute the false discovery rate.[66] Genes with *q*-value ≤0.05 were deemed differentially expressed and submitted to Ingenuity Pathway Analysis (http://www.ingenuity.com) to identify and model the gene networks.

Real-Time PCR

Quantitative real-time PCR (qRT-PCR) for select genes was performed using the Step One Plus real-time PCR system (Life Techonologies, Carlsbad, CA). Total RNA (150 ng) was reverse transcribed with oligo(dT)$_{20}$ primers and Superscript III reverse transcriptase (Life Techonologies, Carlsbad, CA). One microliter of the cDNA was used as template in subsequent qRT-PCR reactions. The qRT-PCR reaction was performed with the Power SYBR Green master mix (Life Techonologies, Carlsbad, CA). The integrity of the PCR reaction was verified by melt curve analysis. All PCR primer sequences are listed in Table 5 of the Supporting Information.

Statistical Analysis

Student's *t* tests, one-way analysis of variance (ANOVA), and repeated measures one-way ANOVA were used for between-group comparisons. Post hoc analysis were conducted using Tukey's test. All data are presented as mean ± SEM.

Supplementary Material

Refer to Web version on PubMed Central for supplementary material.

Acknowledgments

Funding

This work was supported by grants from the National Institute of Diabetes, Digestive and Kidney Diseases [DK095911] to R.T.D., the NIDDK Diabetes Complications Consortium (DiaComp) [DK076169] to R.T.D., the National Cancer Institute [CA120458, CA109265] to B.S.J.B., and the National Institute of Neurologic Diseases [NS075311] to B.S.J.B. and R.T.D. The Genome Sequencing and Bioinformatics Cores are supported by a Center of Biomedical Research Excellence grant [GM103638] and a Kansas Idea Network of Biomedical Research Excellence grant [GM103418] from the National Institute of General Medicine.

ABBREVIATIONS

DPN	diabetic peripheral neuropathy
DRG	dorsal root ganglia
FBG	fasting blood glucose
FCCP	carbonylcyanide-4-(trifluoromethoxy)-phenylhydrazone
FPKM	fragments per kb per million aligned reads
Hsp70	heat shock protein 70
Hsp90	heat shock protein 90

MRC	maximum respiratory capacity
mtBE	mitochondrial bioenergetics
MNCV	motor nerve conduction velocity
OCR	oxygen consumption rate
RNA Seq	RNA sequencing
SNCV	sensory nerve conduction velocity
SRC	spare respiratory capacity
STZ	streptozotocin

REFERENCES

1. Whiting DR, Guariguata L, Weil C, Shaw J. IDF diabetes atlas: Global estimates of the prevalence of diabetes for 2011 and 2030. Diabetes Res. Clin. Pract. 2011; 94:311–321. [PubMed: 22079683]
2. Callaghan BC, Cheng HT, Stables CL, Smith AL, Feldman EL. Diabetic neuropathy: Clinical manifestations and current treatments. Lancet Neurol. 2012; 11:521–534. [PubMed: 22608666]
3. Callaghan BC, Little AA, Feldman EL, Hughes RA. Enhanced glucose control for preventing and treating diabetic neuropathy. Cochrane Database System Rev. 2012; 6 CD007543.
4. Vincent AM, Calabek B, Roberts L, Feldman EL. Biology of diabetic neuropathy. Handbook Clin Neurol. 2013; 115:591–606.
5. Albers JW, Pop-Busui R. Diabetic neuropathy: Mechanisms, emerging treatments, and subtypes. Curr. Neurol. Neurosci. Rep. 2014; 14:473. [PubMed: 24954624]
6. Chowdhury SK, Smith DR, Fernyhough P. The role of aberrant mitochondrial bioenergetics in diabetic neuropathy. Neurobiol. Dis. 2013; 51:56–65. [PubMed: 22446165]
7. Obrosova IG. Diabetes and the peripheral nerve. Biochim. Biophys.. Acta, Mol. Basis Dis. 2009; 1792(10):931–940.
8. Farmer KL, Li C, Dobrowsky RT. Diabetic peripheral neuropathy: Should a chaperone accompany our therapeutic approach? Pharmacol. Rev. 2012; 64:880–900. [PubMed: 22885705]
9. Zochodne DW. Mechanisms of diabetic neuron damage: Molecular pathways. Handbook Clin Neurol. 2014; 126:379–399.
10. Calcutt NA. Tolerating diabetes - An alternative therapeutic approach for diabetic neuropathy. ASN Neuro. 2010; 2:215–217.
11. Vihervaara A, Sistonen L. HSF1 at a glance. J. Cell Sci. 2014; 127:261–266. [PubMed: 24421309]
12. Luo W, Dou F, Rodina A, Chip S, Kim J, Zhao Q, Moulick K, Aguirre J, Wu N, Greengard P, Chiosis G. Roles of heat-shock protein 90 in maintaining and facilitating the neurodegenerative phenotype in tauopathies. Proc. Natl. Acad. Sci. U. S. A. 2007; 104:9511–9516. [PubMed: 17517623]
13. Dickey CA, Kamal A, Lundgren K, Klosak N, Bailey RM, Dunmore J, Ash P, Shoraka S, Zlatkovic J, Eckman CB, Patterson C, Dickson DW, Nahman NS Jr, Hutton M, Burrows F, Petrucelli L. The high-affinity Hsp90-Chip complex recognizes and selectively degrades phosphorylated tau client proteins. J. Clin. Invest. 2007; 117:648–658. [PubMed: 17304350]
14. Waza M, Adachi H, Katsuno M, Minamiyama M, Sang C, Tanaka F, Inukai A, Doyu M, Sobue G. 17-AAG, an Hsp90 inhibitor, ameliorates polyglutamine-mediated motor neuron degeneration. Nat. Med. 2005; 11:1088–1095. [PubMed: 16155577]
15. Morimoto RI. The heat shock response: Systems biology of proteotoxic stress in aging and disease. Cold Spring Harbor Symp. Quant. Biol. 2011; 76:91–99. [PubMed: 22371371]
16. Chittoor-Vinod VG, Lee S, Judge SM, Notterpek L. Inducible Hsp70 is critical in preventing the aggregation and enhancing the processing of PMP22. ASN Neuro. 2015; 7 1759091415569909.

17. Urban MJ, Li C, Yu C, Lu Y, Krise JM, McIntosh MP, Rajewski RA, Blagg BSJ, Dobrowsky RT. Inhibiting heat shock protein 90 reverses sensory hypoalgesia in diabetic mice. ASN Neuro. 2010; 2:189–199.
18. Li C, Ma J, Zhao H, Blagg BSJ, Dobrowsky RT. Induction of heat shock protein 70 (Hsp70) prevents neuregulin-induced demyelination by enhancing the proteasomal clearance of c-jun. ASN Neuro. 2012; 4:425–437.
19. Zhang L, Zhao H, Blagg BS, Dobrowsky RT. A C-terminal heat shock protein 90 inhibitor decreases hyperglycemia-induced oxidative stress and improves mitochondrial bioenergetics in sensory neurons. J. Proteome Res. 2012; 11:2581–2593. [PubMed: 22413817]
20. Kusuma BR, Zhang L, Sundstrom T, Peterson LB, Dobrowsky RT, Blagg BSJ. Synthesis and evaluation of novologues as C-terminal Hsp90 inhibitors with cytoprotective activity against sensory neuron glucotoxicity. J. Med. Chem. 2012; 55:5797–5812. [PubMed: 22702513]
21. Ma J, Farmer KL, Pan P, Urban MJ, Zhao H, Blagg BS, Dobrowsky RT. Heat shock protein 70 is necessary to improve mitochondrial bioenergetics and reverse diabetic sensory neuropathy following KU-32 therapy. J. Pharmacol. Exp. Ther. 2014; 348:281–292. [PubMed: 24263156]
22. Evans CG, Chang L, Gestwicki JE. Heat shock protein 70 (Hsp70) as an emerging drug target. J. Med. Chem. 2010; 53:4585–4602. [PubMed: 20334364]
23. Hinder LM, Vivekanandan-Giri A, McLean LL, Pennathur S, Feldman EL. Decreased glycolytic and tricarboxylic acid cycle intermediates coincide with peripheral nervous system oxidative stress in a murine model of type 2 diabetes. J. Endocrinol. 2013; 216:1–11. [PubMed: 23086140]
24. Pande M, Hur J, Hong Y, Backus C, Hayes JM, Oh SS, Kretzler M, Feldman EL. Transcriptional profiling of diabetic neuropathy in the BKS db/db mouse: A model of type 2 diabetes. Diabetes. 2011; 60:1981–1989. [PubMed: 21617178]
25. Hur J, Sullivan KA, Pande M, Hong Y, Sima AAF, Jagadish HV, Kretzler M, Feldman EL. The identification of gene expression profiles associated with progression of human diabetic neuropathy. Brain. 2011; 134:3222–3235. [PubMed: 21926103]
26. Wang Z, Gerstein M, Snyder M. RNA-Seq: A revolutionary tool for transcriptomics. Nat. Rev. Genet. 2009; 10:57–63. [PubMed: 19015660]
27. Mortazavi A, Williams BA, McCue K, Schaeffer L, Wold B. Mapping and quantifying mammalian transcriptomes by RNA-Seq. Nat. Methods. 2008; 5:621–628. [PubMed: 18516045]
28. Urban MJ, Pan P, Farmer KL, Zhao H, Blagg BS, Dobrowsky RT. Modulating molecular chaperones improves sensory fiber recovery and mitochondrial function in diabetic peripheral neuropathy. Exp. Neurol. 2012; 235:388–396. [PubMed: 22465570]
29. Navarro JF, Mora C. Role of inflammation in diabetic complications. Nephrol., Dial., Transplant. 2005; 20:2601–2604. [PubMed: 16188894]
30. Huang C, Wang J, Chen Z, Wang Y, Zhang W. 2-Phenylethynesulfonamide prevents induction of pro-inflammatory factors and attenuates LPS-induced liver injury by targeting NHE1-Hsp70 complex in mice. PLoS One. 2013; 8:e67582. [PubMed: 23805318]
31. Senf SM, Howard TM, Ahn B, Ferreira LF, Judge AR. Loss of the inducible Hsp70 delays the inflammatory response to skeletal muscle injury and severely impairs muscle regeneration. PLoS One. 2013; 8:e62687. [PubMed: 23626847]
32. Hunter-Lavin C, Davies EL, Bacelar MM, Marshall MJ, Andrew SM, Williams JH. Hsp70 release from peripheral blood mononuclear cells. Biochem. Biophys. Res. Commun. 2004; 324:511–517. [PubMed: 15474457]
33. Krause M, Heck TG, Bittencourt A, Scomazzon SP, Newsholme P, Curi R, Homem de Bittencourt PI Jr. The chaperone balance hypothesis: The importance of the extracellular to intracellular Hsp70 ratio to inflammation-driven Type 2 diabetes, the effect of exercise, and the implications for clinical management. Mediators Inflammation. 2015; 2015:249205.
34. Mansilla MJ, Costa C, Eixarch H, Tepavcevic V, Castillo M, Martin R, Lubetzki C, Aigrot MS, Montalban X, Espejo C. Hsp70 regulates immune response in experimental autoimmune encephalomyelitis. PLoS One. 2014; 9:e105737. [PubMed: 25153885]
35. Whitham M, Fortes MB. Heat shock protein 72: Release and biological significance during exercise. Front. Biosci., Landmark Ed. 2008; 13:1328–1339.

36. Jones Q, Voegeli TS, Li G, Chen Y, Currie RW. Heat shock proteins protect against ischemia and inflammation through multiple mechanisms. Inflammation Allergy: Drug Targets. 2011; 10:247–259. [PubMed: 21539516]
37. Rodrigues-Krause J, Krause M, O'Hagan C, De Vito G, Boreham C, Murphy C, Newsholme P, Colleran G. Divergence of intracellular and extracellular Hsp72 in Type 2 diabetes: Does fat matter? Cell Stress Chaperones. 2012; 17:293–302. [PubMed: 22215518]
38. Kristiansen M, Graversen JH, Jacobsen C, Sonne O, Hoffman HJ, Law SK, Moestrup SK. Identification of the haemoglobin scavenger receptor. Nature. 2001; 409:198–201. [PubMed: 11196644]
39. Nukada H, McMorran PD, Baba M, Ogasawara S, Yagihashi S. Increased susceptibility to ischemia and macrophage activation in STZ-diabetic rat nerve. Brain Res. 2011; 1373:172–182. [PubMed: 21134361]
40. Kallestrup M, Müller HJ, Tankisi H, Andersen H. Soluble CD163 levels are elevated in cerebrospinal fluid and serum in people with Type 2 diabetes mellitus and are associated with impaired peripheral nerve function. Diabet Med. 2015; 32:54–61. [PubMed: 25156085]
41. O'Brien PD, Hur J, Hayes JM, Backus C, Sakowski SA, Feldman EL. BTBR ob/ob mice as a novel diabetic neuropathy model: Neurological characterization and gene expression analyses. Neurobiol. Dis. 2015; 73:348–355.
42. Ortmann KL, Chattopadhyay M. Decrease in neuroimmune activation by HSV-mediated gene transfer of TNFalpha soluble receptor alleviates pain in rats with diabetic neuropathy. Brain, Behav., Immun. 2014; 41:144–151. [PubMed: 24880032]
43. Yoon H, Thakur V, Isham D, Fayad M, Chattopadhyay M. Moderate exercise training attenuates inflammatory mediators in DRG of Type 1 diabetic rats. Exp. Neurol. 2015; 267:107–114. [PubMed: 25783659]
44. Dominguez JM 2nd, Yorek MA, Grant MB. Combination therapies prevent the neuropathic, proinflammatory characteristics of bone marrow in streptozotocin-induced diabetic rats. Diabetes. 2015; 64:643–653. [PubMed: 25204979]
45. Nicholson A, Reifsnyder PC, Malcolm RD, Lucas CA, MacGregor GR, Zhang W, Leiter EH. Diet-induced obesity in two C57Bl/6 substrains with intact or mutant nicotinamide nucleotide transhydrogenase (nnt) gene. Obesity. 2010; 18:1902–1905. [PubMed: 20057372]
46. Ronchi JA, Figueira TR, Ravagnani FG, Oliveira HCF, Vercesi AE, Castilho RF. A spontaneous mutation in the nicotinamide nucleotide transhydrogenase gene of C57Bl/6J mice results in mitochondrial redox abnormalities. Free Radical Biol. Med. 2013; 63:446–456. [PubMed: 23747984]
47. Vincent AM, Russell JW, Low P, Feldman EL. Oxidative stress in the pathogenesis of diabetic neuropathy. Endocr. Rev. 2004; 25:612–628. [PubMed: 15294884]
48. Figueroa-Romero C, Sadidi M, Feldman EL. Mechanisms of disease: The oxidative stress theory of diabetic neuropathy. Rev. Endocr. Metab. Disord. 2008; 9:301–314. [PubMed: 18709457]
49. Kasznicki J, Kosmalski M, Sliwinska A, Mrowicka M, Stanczyk M, Majsterek I, Drzewoski J. Evaluation of oxidative stress markers in pathogenesis of diabetic neuropathy. Mol. Biol. Rep. 2012; 39:8669–8678. [PubMed: 22718504]
50. Edwards JL, Vincent AM, Cheng HT, Feldman EL. Diabetic neuropathy: Mechanisms to management. Pharmacol. Ther. 2008; 120:1–34. [PubMed: 18616962]
51. Tammariello SP, Quinn MT, Estus S. NADPH oxidase contributes directly to oxidative stress and apoptosis in nerve growth factor-deprived sympathetic neurons. J. Neurosci. 2000; 20:RC53. [PubMed: 10627630]
52. Devi TS, Lee I, Huttemann M, Kumar A, Nantwi KD, Singh LP. Txnip links innate host defense mechanisms to oxidative stress and inflammation in retinal muller glia under chronic hyperglycemia: Implications for diabetic retinopathy. Exp. Diabetes Res. 2012; 2012:438238. [PubMed: 22474421]
53. Schulze PC, Yoshioka J, Takahashi T, He Z, King GL, Lee RT. Hyperglycemia promotes oxidative stress through inhibition of thioredoxin function by thioredoxin-interacting protein. J. Biol. Chem. 2004; 279:30369–30374. [PubMed: 15128745]

54. Broome CS, Kayani AC, Palomero J, Dillmann WH, Mestril R, Jackson MJ, McArdle A. Effect of lifelong overexpression of Hsp70 in skeletal muscle on age-related oxidative stress and adaptation after nondamaging contractile activity. FASEB J. 2006; 20:1549–1551. [PubMed: 16723383]
55. Akude E, Zherebitskaya E, Chowdhury SKR, Smith DR, Dobrowsky RT, Fernyhough P. Diminished superoxide generation is associated with respiratory chain dysfunction and changes in the mitochondrial proteome of sensory neurons from diabetic rats. Diabetes. 2011; 60:288–297. [PubMed: 20876714]
56. Lee I, Huttemann M. Energy crisis: The role of oxidative phosphorylation in acute inflammation and sepsis. Biochim. Biophys. Acta, Mol. Basis Dis. 2014; 1842:1579–1586.
57. Margineantu DH, Emerson CB, Diaz D, Hockenbery DM. Hsp90 inhibition decreases mitochondrial protein turnover. PLoS One. 2007; 2:e1066. [PubMed: 17957250]
58. Fierro-Monti I, Racle J, Hernandez C, Waridel P, Hatzimanikatis V, Quadroni M. A novel pulse-chase SILAC strategy measures changes in protein decay and synthesis rates induced by perturbation of proteostasis with an Hsp90 inhibitor. PLoS One. 2013; 8:e80423. [PubMed: 24312217]
59. Quadroni M, Potts A, Waridel P. Hsp90 inhibition induces both protein-specific and global changes in the ubiquitinome. J. Proteomics. 2015; 120:215–229. [PubMed: 25782750]
60. McGuire JF, Rouen S, Siegfreid E, Wright DE, Dobrowsky RT. Caveolin-1 and altered neuregulin signaling contribute to the pathophysiological progression of diabetic peripheral neuropathy. Diabetes. 2009; 58:2677–2686. [PubMed: 19675140]
61. Brand MD, Nicholls DG. Assessing mitochondrial dysfunction in cells. Biochem. J. 2011; 435:297–312. [PubMed: 21726199]
62. Roy Chowdhury SK, Smith DR, Saleh A, Schapansky J, Marquez A, Gomes S, Akude E, Morrow D, Calcutt NA, Fernyhough P. Impaired adenosine monophosphate-activated protein kinase signalling in dorsal root ganglia neurons is linked to mitochondrial dysfunction and peripheral neuropathy in diabetes. Brain. 2012; 135:1751–1766. [PubMed: 22561641]
63. Goecks J, Nekrutenko A, Taylor J. The Galaxy Team Galaxy: A comprehensive approach for supporting accessible, reproducible, and transparent computational research in the life sciences. Genome Biol. 2010; 11:R86. [PubMed: 20738864]
64. Trapnell C, Hendrickson DG, Sauvageau M, Goff L, Rinn JL, Pachter L. Differential analysis of gene regulation at transcript resolution with RNA-Seq. Nat. Biotechnol. 2013; 31:46–53. [PubMed: 23222703]
65. Trapnell C, Roberts A, Goff L, Pertea G, Kim D, Kelley DR, Pimentel H, Salzberg SL, Rinn JL, Pachter L. Differential gene and transcript expression analysis of RNA-Seq experiments with Tophat and Cufflinks. Nat. Protoc. 2012; 7:562–578. [PubMed: 22383036]
66. Rapaport F, Khanin R, Liang Y, Pirun M, Krek A, Zumbo P, Mason CE, Socci ND, Betel D. Comprehensive evaluation of differential gene expression analysis methods for RNA-Seq data. Genome Biol. 2013; 14:R95. [PubMed: 24020486]

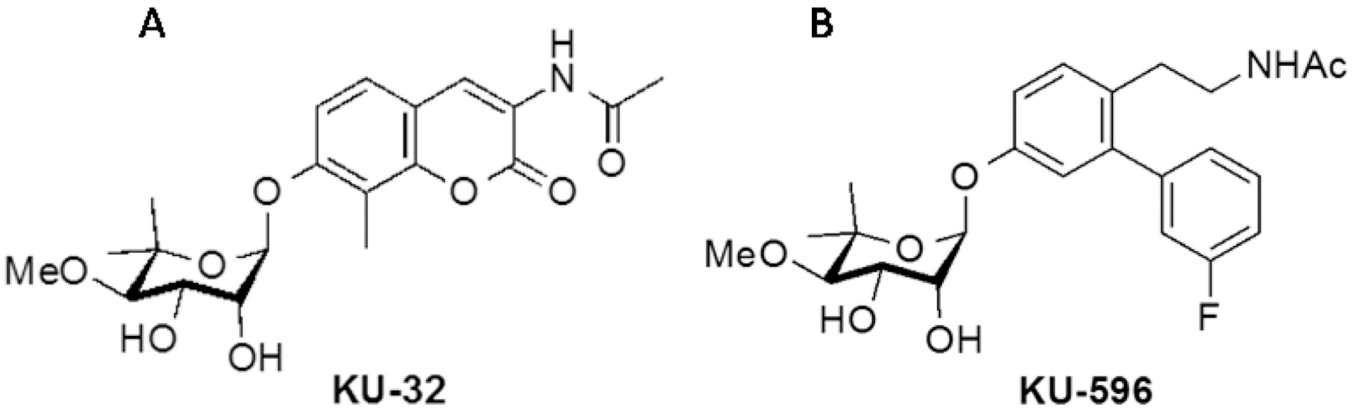

Figure 1.
Structure of (A) KU-32 and (B) the novologue KU-596. The B-ring is fluorinated.

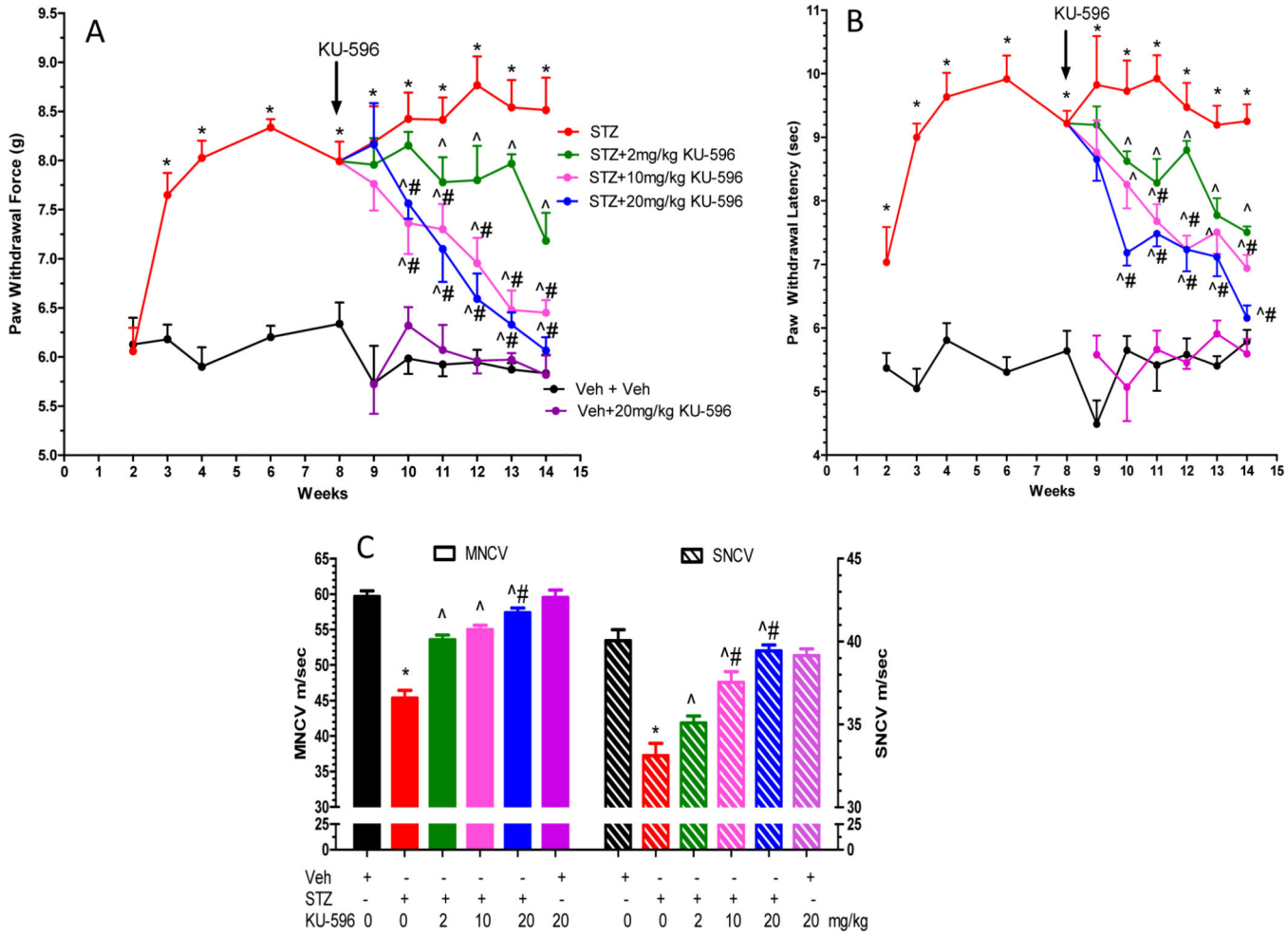

Figure 2.

Dose response of KU-596 in reversing mechanical (A) and thermal (B) hypoalgesia. (C) KU-596 attenuated deficits in motor and sensory nerve conduction velocity. *$p < 0.05$ vs Veh+Veh; ^$p < 0.05$ vs STZ + Veh; $^{\#}p < 0.05$ vs time-matched STZ + 2 mg/kg KU-596.

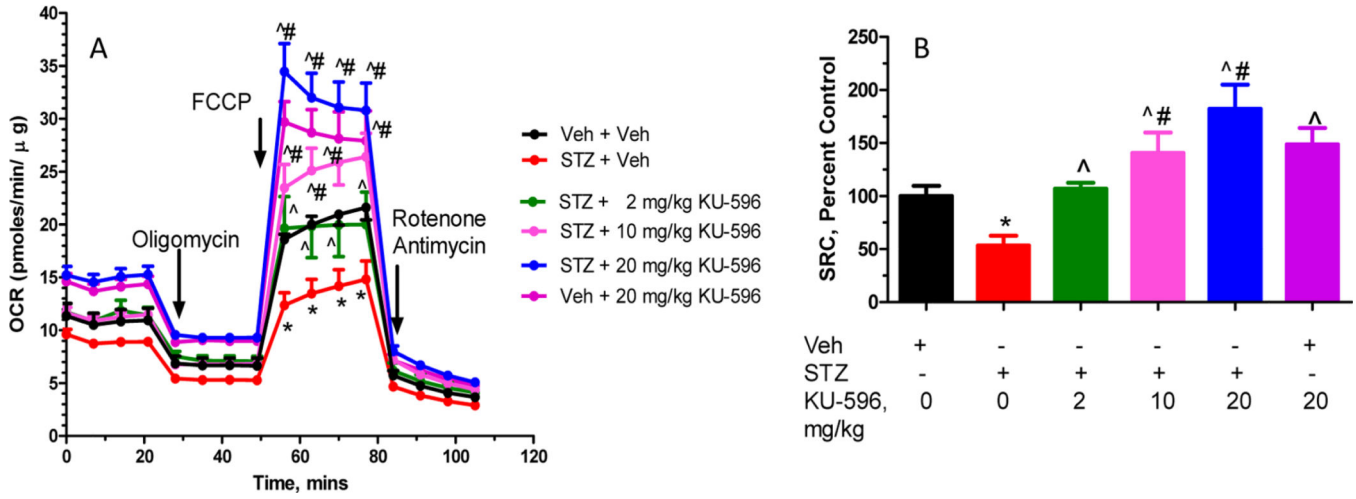

Figure 3.

(A) KU-596 improved MRC in the sensory neurons of diabetic mice in a dose-dependent manner. (B) Spare respiratory capacity (SRC) was quantified and expressed as percent of the control group (Veh + Veh). *$p < 0.05$ vs Veh + Veh; ^$p < 0.05$ vs STZ + Veh; $^{\#}p < 0.05$ vs STZ + 2 mg/kg KU-596.

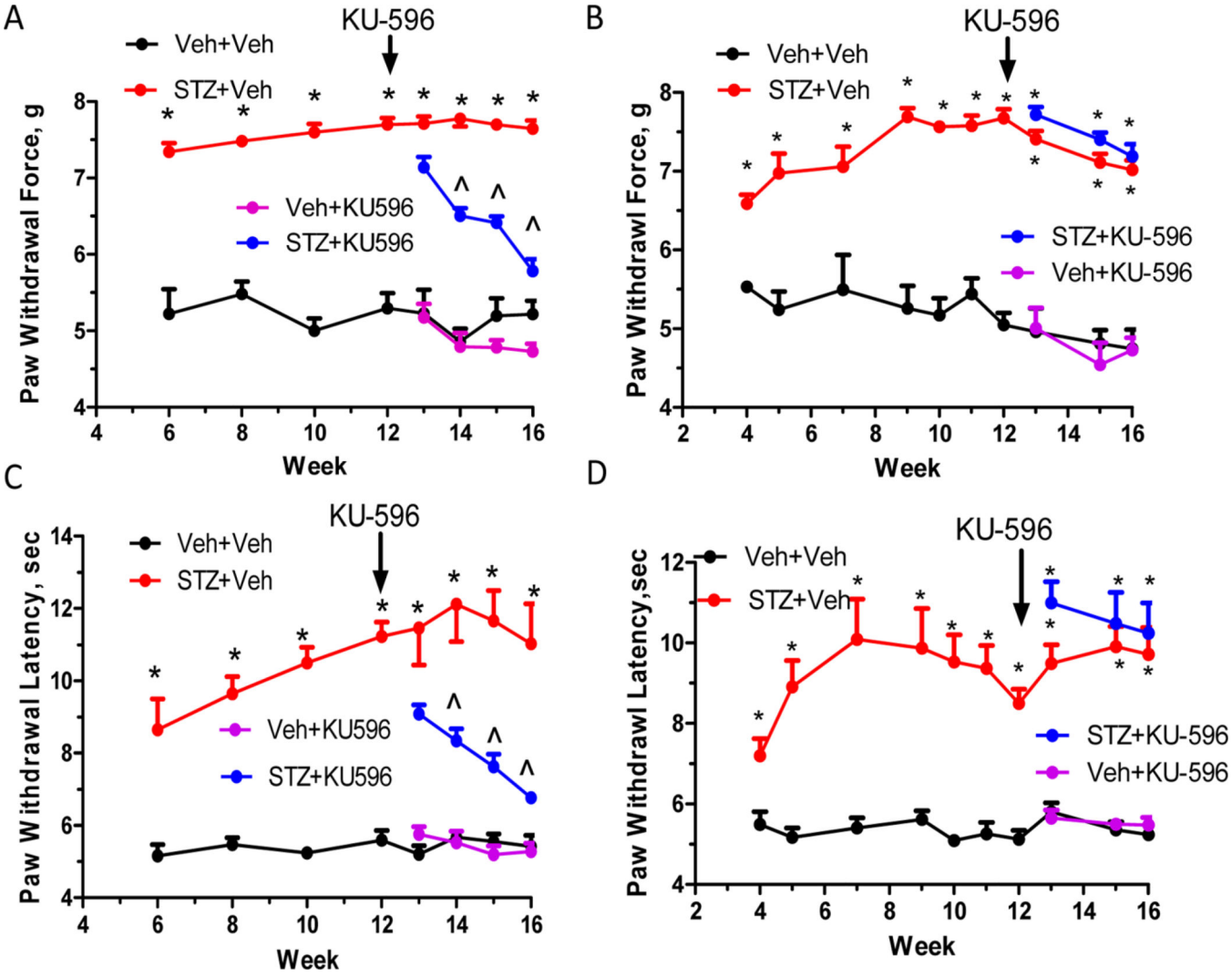

Figure 4.

KU-596 reverses sensory deficits in diabetic mice in an Hsp70-dependent manner. Diabetic WT (A,C) and Hsp70 KO (B,D) mice showed little difference in the temporal onset or magnitude of the sensory hypoalgesia. KU-596 treatment was initiated after 12 weeks of diabetes, and mechanical (A) and thermal (C) hypoalgesia were partially reversed over 4 weeks in C57Bl/6 mice. In contrast, drug treatment did not reverse either the mechanical (B) or thermal (D) hypoalgesia in the Hsp70 KO mice. *$p < 0.05$ vs Veh + Veh; ^$p < 0.05$ vs time-matched STZ + Veh.

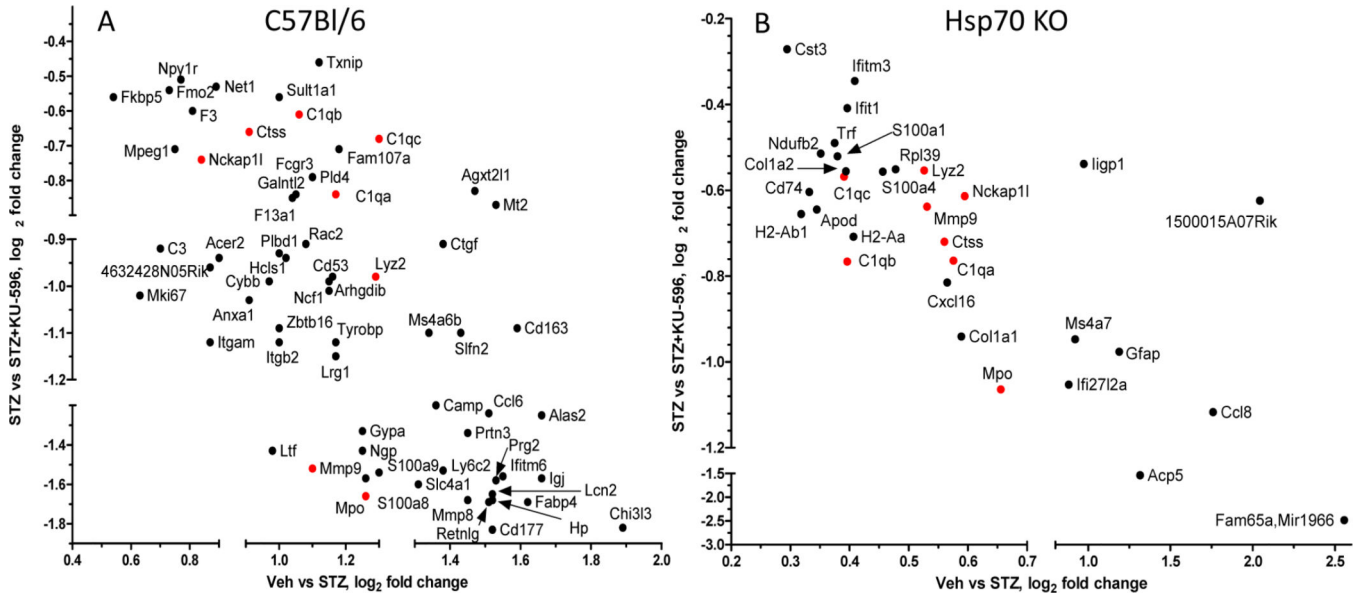

Figure 5.

KU-596 therapy normalized the expression of numerous genes in a Hsp70 independent manner. The $\log_2$ fold change of genes that were detected in diabetic WT (A) and Hsp70 KO (B) mice in the absence (abscissa) and presence (ordinate) of KU-596 were plotted. Genes in red were altered in both the diabetic WT and Hsp70 KO mice.

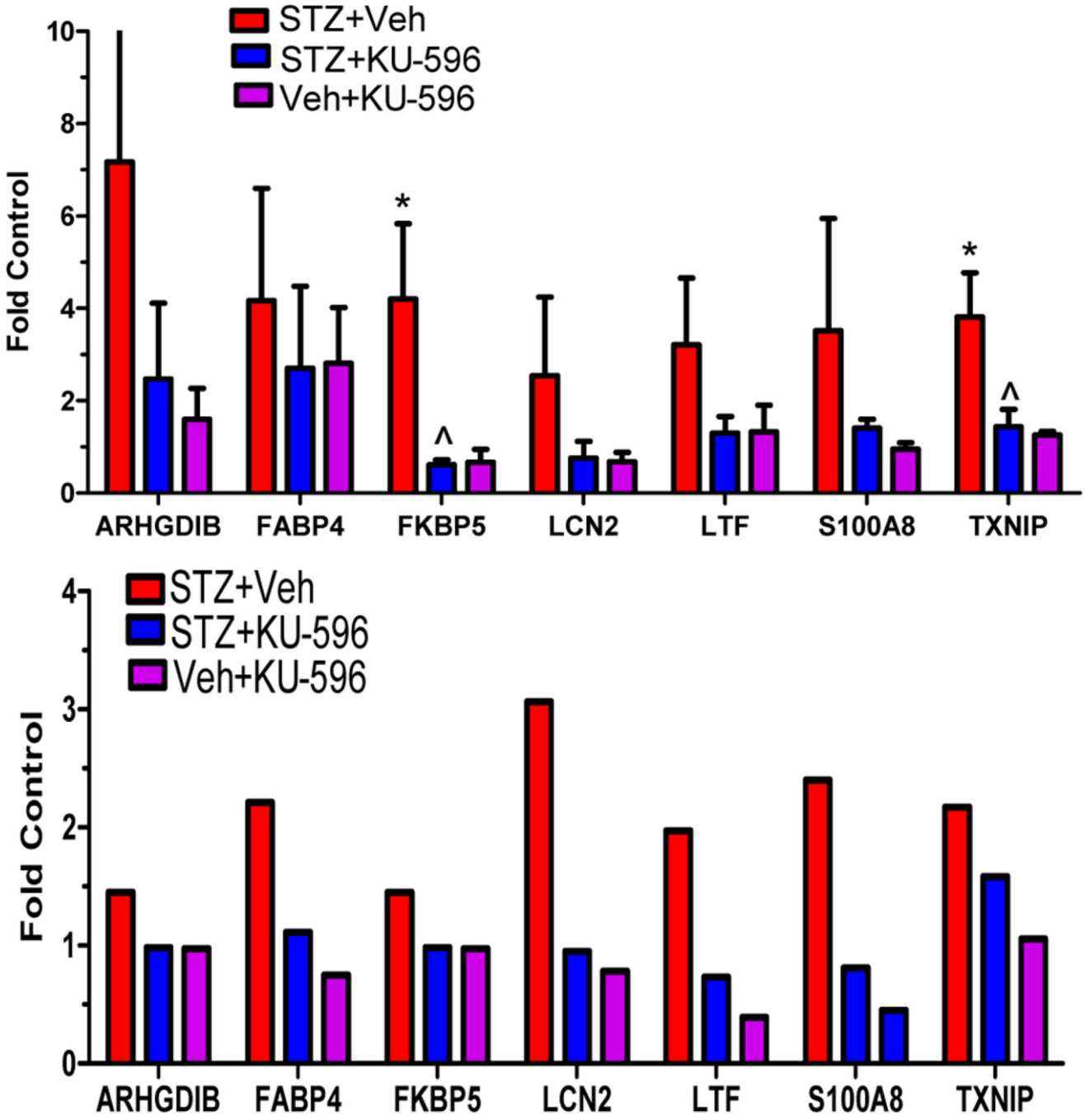

Figure 6.

qRT-PCR validation of RNA-Seq data in C57Bl/6 mice. (A) Total RNA was prepared for mRNA quantification by standard qRT-PCR. Tubulin was used as the internal control. The data were expressed as fold change versus nondiabetic mice for each gene. *$p < 0.05$ vs Veh + Veh; ^$p < 0.05$ vs STZ + Veh; $n = 3$. (B) Fold change versus nondiabetic mice using the normalized FPKM values from RNA-Seq

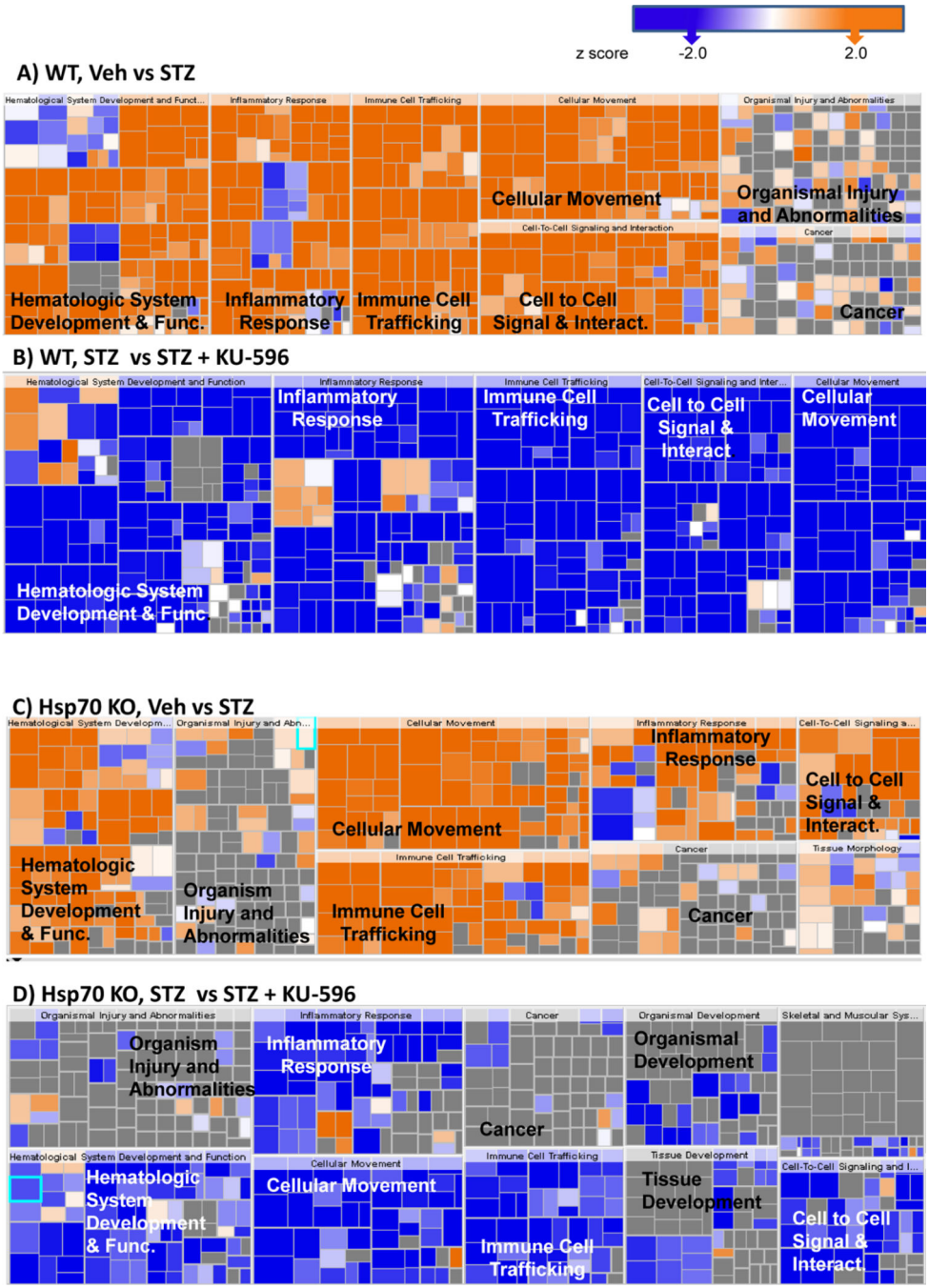

Figure 7.

Significantly altered biologic processes in WT (A, B) and Hsp70 KO mice (C, D). In both genotypes, diabetes activated inflammatory responses (A, C), and these were decreased by novologue treatment (B, D). The size of each box represents the negative log of the *p*-value of the genes associated with each biologic process, indicating enrichment. The color of each box indicates the activation *z*-scores; ≥2 (orange, activated) or ≤ −2 (blue, inhibited), gray, no effect.

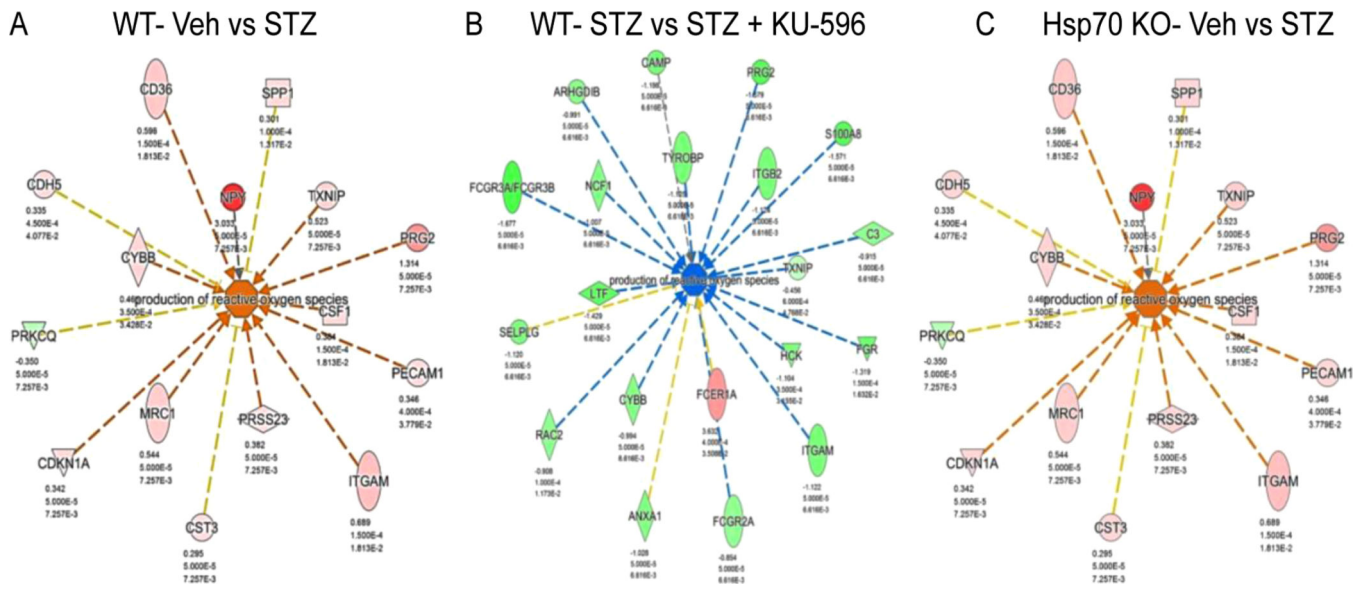

Figure 8.

Genes involved in ROS production were increased in diabetic WT (A, B) and Hsp70 KO mice (C). WT Veh vs STZ + Veh (A) and STZ vs STZ + KU-596 (B). Hsp70 KO Veh vs STZ (C). Novologue therapy was only predicted to decrease this biologic process in diabetic WT mice. Red indicates upregulation of the molecules, and green indicates downregulation. Greater node color intensity corresponds to a higher level of change in expression. Edge color represent the predicted effects on the production of ROS: orange, activation; blue, inhibition; yellow, inconsistent with the activation state of the downstream molecule; gray, an effect is not predicted.

Table 1

Weight, FBG, and HbA1c of Swiss Webster Mice

treatment[a]	weight, g	FBG, mg/dL	HbA1c, % (mmol/mol)[b]	*n*
Veh + Veh	35.6 ± 2.4	153 ± 42	5.2 ± 0.1 (33.3 ± 1.1)	6
STZ + Veh	27.9 ± 2.2[c]	596 ± 7[c]	13.0 ± 0[c,d] (118.6 ± 0)	5
STZ + 2 mg/kg KU-596	30.4 ± 2.5[c]	554 ± 113[c]	12.6 ± 0.6[c] (114.2 ± 6.6)	6
STZ + 10 mg/kg KU-596	30.6 ± 2.1[c]	525 ± 128[c]	11.9 ± 1.3[c] (106.6 ± 14.3)	7
STZ + 20 mg/kg KU-596	29.0 ± 2.0[c]	600 ± 0[c,d]	12.9 ± 0.1[c] (117.5 ± 1.1)	7
Veh + 20 mg/kg KU-596	34.1 ± 1.4	128 ± 10	5.1 ± 0.2 (32.2 ± 0.2)	7

[a] Veh, vehicle; STZ, streptozotocin.

[b] mmol of HbA1c/mol of hemoglobin.

[c] $p < 0.05$ versus Veh + Veh. Veh for STZ was 0.1 M sodium citrate in PBS, pH 4.5; Veh for KU-596 was 0.1 M Captisol in water.

[d] Maximal reading.

Table 2

Weight, FBG, and HbA1c of C57Bl/6 and Hsp70 KO Mice

	C57Bl/6				Hsp70 KO			
treatment[a]	**weight, g**	**FBG, mg/dL**	**HbA1c, % (mmol/mol)**[b]	***n***	**weight, g**	**FBG, mg/dL**	**HbA1c, % (mmol/mol)**[b]	***n***
Veh + Veh	34.6 ± 6.7	145 ± 12	4.6 ± 0.2 (26.8 ± 2.2)	7	28.1 ± 5.5	177 ± 20	5.0 ± 0.3 (31.1 ± 3.3)	9
STZ + Veh	22.6 ± 2.0[c]	540 ± 48[c]	9.1 ± 1.3[c] (76.0 ± 14.3)	6	23.2 ± 3.0[c]	524 ± 80[c]	11.1 ± 3.3[c] (97.8 ± 36.3)	10
STZ + KU-596	25.1 ± 3.2[c]	499 ± 82[c]	9.3 ± 2.7[c] (78.1 ± 29.7)	7	22.0 ± 2.8[c]	573 ± 22[c]	10.3 ± 2.4[c] (89.1 ± 26.4)	9
Veh + KU-596	33.9 ± 4.5	157 ± 20	4.4 ± 0.2 (24.6 ± 2.2)	7	27.0 ± 5.1	168 ± 19	5.2 ± 0.2 (33.3 ± 0.2)	8

[a] Veh, vehicle; STZ, streptozotocin.

[b] mmol of HbA1c/mol of hemoglobin.

[c] $p < 0.05$ versus Veh + Veh. Veh for STZ was 0.1 M sodium citrate in PBS, pH 4.5; Veh for KU-596 was 0.1 M Captisol in water.